Harri Kosonen, Sami Valkama, Janne Ruokolainen, Mika Torkkeli, Ritva Serimaa, Gerrit ten Brinke, and Olli Ikkala. One-Dimensional Optical Reflectors Based on Self-Organization of Polymeric Comb-Shaped Supramolecules, The European Physical Journal E 2003, 10, 69-75.

Eur. Phys. J. E **10**, 69–75 (2003)
DOI: 10.1140/epje/e2003-00007-0

THE EUROPEAN PHYSICAL JOURNAL E

One-dimensional optical reflectors based on self-organization of polymeric comb-shaped supramolecules

H. Kosonen[1,2], S. Valkama[1], J. Ruokolainen[1,3], M. Torkkeli[4], R. Serimaa[4], G. ten Brinke[1,5,a], and O. Ikkala[1,b]

[1] Department of Engineering Physics and Mathematics and Center for New Materials, Helsinki University of Technology, PO Box 2200, FIN-02015 HUT, Espoo, Finland
[2] VTT Microelectronics, Technical Research Centre of Finland, PO Box 1208, FIN-02044 VIT, Finland
[3] Department of Materials, University of California Santa Barbara, Santa Barbara, CA 93106 USA
[4] Department of Physical Sciences, University of Helsinki, PO Box 64, FIN-00014 Helsinki, Finland
[5] Laboratory of Polymer Chemistry, Dutch Polymer Institute, University of Groningen, Nijenborgh 4, 9747 AG Groningen, The Netherlands

Received 30 April 2002
Published online: 11 March 2003 –

Abstract. We demonstrate that complexation of dodecylbenzenesulphonic acid, DBSA, to a diblock copolymer of polystyrene-*block*-poly(4-vinylpyridine), PS-*block*-P4VP, leads to polymeric supramolecules PS-*block*-P4VP(DBSA)$_y$ ($y = 1.0$, 1.5, and 2.0), which self-organize with a particularly large lamellar periodicity in excess of 1000 Å. The structures consist of alternating PS and P4VP(DBSA)$_y$ layers, where the latter contains smaller internal structure, probably lamellar. The DBSA side chains are bonded to the pyridines by protonation and hydrogen bonding and they effectively plasticize the material. In this way relatively well-developed structures are obtained even without annealing or macroscopic alignment. Transmission and reflectance measurements show that a relatively narrow and incomplete bandgap exists for supramolecules of high molecular weight block copolymer at *ca.* 460 nm.

PACS. 42.70.Qs Photonic bandgap materials – 83.70.Hq Heterogeneous liquids: suspensions, dispersions, emulsions, pastes, slurries, foams, block copolymers, etc.

1 Introduction

There has been considerable interest over the recent years to develop periodic dielectric structures to manipulate the flow of light [1–4]. If properly periodic 3D structures at the optical wavelengths and sufficient dielectric contrast between the ordered domains can be prepared, propagation of light at the matching wavelengths can be blocked, thus leading to complete photonic bandgap. In combination with controlled defect structures, a wealth of applications in photonics is expected.

Such photonic crystals have turned out to be difficult to construct. Lithographic and etching techniques, in principle, make it possible to engineer structures and defects in detail, as well as to attain sufficient dielectric contrast, but achievement of small structures down to the optical length scale is challenging. On the other hand, spontaneous assemblies allow formation of small enough structures based on colloids [5,6], synthetic opals [7–11], inverted opals [7,12–16], and block copolymers [17–22]. In such cases, although the organization leads to a well-defined local order, it is nontrivial to achieve perfectly ordered structures over the macroscopic length scale, which, in addition should contain carefully engineered defects for "light channels". Therefore, it may turn out that self-assembly leads to new, more robust applications where a complete photonic bandgap and detailed engineering of defects are not required, but still strong interaction with light at given wavelengths is needed.

Block copolymers typically form self-organized lamellar (1D), cylindrical (2D), spherical, and gyroid (3D) structures typically at a length scale of 100–1000 Å, *i.e.* smaller than the optical length scale [23,24]. Increase in the long period up to 1000–2000 Å range, corresponding to $\lambda/2n$ for optical wavelengths, could in principle, be achieved just by using block copolymers of higher molecular weight. This, however, would lead to excessively slow structure formation and poor structures are expected. This has been overcome by swelling the block copolymer domains with narrow molecular weight homopolymers or oligomeric plasticizers [18,20,21]. In this way, incomplete photonic bandgaps have been constructed where increased dielectric contrast has been achieved in some cases by incorporating suitable high refractive index inorganic additives within the domains [17].

We have previously shown that comb-shaped polymeric supramolecules [25–27], consisting of hydrogen

[a] e-mail: g.ten.Brinke@chem.rug.nl
[b] e-mail: Olli.Ikkala@hut.fi

bonded "combs" (alkyl phenols) within one block of a polystyrene-*block*-poly(4-vinylpyridine) diblock copolymer lead to structure-*within*-structure self-organization with particularly long periodicities due to stretching of the chains. Long periods of *ca.* 1400 Å were reported [27]. The samples turned predominantly blue pearlescent to an observer viewing it in ambient. Importantly the structure formation is particularly facile as the hydrogen bonded phenolic side chains, in addition of being constituents of the supramolecules, simultaneously act as plasticizers. This may offer significant benefits, since block copolymers usually demand specific procedures to obtain well-developed local structures. Such observations encouraged us to investigate our comb-shaped supramolecules in more detail in relation to photonic bandgaps. In addition, the structures allow further benefits over the block copolymer/homopolymer blends as in the present case homopolymers with narrow molecular weight distributions are not required. Instead of attaching "combs" by hydrogen bonding, we selected bonding *via* protonation, because it was observed previously that in the case of polyionenes high refractive indexes might be achieved using quaternized nitrogen [28].

Based on these arguments, we selected polystyrene-*block*-poly(4-vinylpyridine) with dodecylbenzenesulphonic acid (DBSA) "combs". In the stoichiometric composition PS-*block*-P4VP(DBSA)$_{1.0}$, DBSA-molecules are expected to be bonded to the pyridines by protonation and further DBSA can be hydrogen bonded to the sulphonates of the inner P4VP(DBSA)$_{1.0}$ layer.

2 Experimental section

2.1 Materials

Two PS-*block*-P4VP diblock copolymers were supplied by Polymer Source Inc. and they were used without further purification; a high molecular weight ($M_{n,\mathrm{PS}}$ = 238,100 g/mol, $M_{n,\mathrm{P4VP}}$ = 49,500 g/mol, M_w/M_n = 1.23) and a low molecular weight ($M_{n,\mathrm{PS}}$ = 42,100 g/mol, $M_{n,\mathrm{P4VP}}$ = 8,100 g/mol, M_w/M_n = 1.08). Note that weight fraction of P4VP in both high and low molecular weight block copolymers is almost the same (*ca.* w = 0.17), *i.e.* leading to complexes with equal weight fractions. Dodecylbenzenesulphonic acid (DBSA) was of purity 90% and it was purchased from Tokyo Kasei.

2.2 Sample preparation

Both PS-*block*-P4VP and DBSA were dissolved in chloroform (Riedel-de Häen, 99%) separately and the solutions were clear and homogenous at the resolution of optical microscope. The solutions were combined leading to complexes PS-*block*-P4VP(DBSA)$_y$. Here y denotes the number of DBSA groups *vs.* 4-vinylpyridine repeat unit (y = 0, 1.0, 1.5, and 2.0). Solutions were stirred 24 hours and the solvent was slowly evaporated at 4 °C (about one week). Thereafter the samples were vacuum dried at 60 °C for 48 hours. Annealing was not performed due to the risk of degradation caused by free sulphonic acid (when $y > 1.0$ there is more sulphonic acid groups than 4-vinylpyridine repeat units).

2.3 Fourier transformation infrared spectroscopy

The interaction between the P4VP block of PS-*block*-P4VP and DBSA was studied using Nicolet Magna 750 FTIR-spectrometer at room temperature. A minimum of 64 scans were averaged at a resolution of 2 cm^{-1}. The samples were analyzed from films cast on potassium bromide crystals. The solvent was evaporated in vacuum at 30 °C for 24 hours.

2.4 X-ray scattering

X-ray scattering was used to study the mesomorphic behaviour of the samples. Most of the experiments were performed with a conventional sealed X-ray tube. The CuK$_\alpha$ radiation (λ = 1.54 Å) was monochromatized by means of totally reflecting mirror (Huber small-angle chamber 701) and Ni-filter. Sample to detector distances of 80, 170, and 1250 mm were used. Together, they span q-range ($q = 4\pi \sin\theta/\lambda$) between 0.008 and 2.0 Å^{-1}. A 2D area detector (Bruker AXS) was used. Additional measurements were performed at the high-brilliance beamline ID2 of the European Synchrotron Radiation Facility (ESRF). The station has undulator source and focusing X-ray optics. At 12.46 keV (λ = 0.995 Å) the flux of photons is about 10^{12} ph/s across the 0.2 * 0.2 mm^2 size beam. The distance between sample and detector was 10 m. The accessible scattering vector lengths range from 0.004 to 0.056 Å^{-1}. The detector was an X-ray image intensifier (TH 49-427) lens coupled to the ESRF developed 2D CCD camera.

2.5 Transmission electron microscopy

Bulk samples of PS-*block*-P4VP(DBSA)$_y$ for TEM characterization were embedded in epoxy and cured at 60 °C overnight. Ultra thin sections (approximately 70 nm) were cryomicrotomed from the embedded specimen using a Leica Ultracut UCT- ultramicrotome and a Diatome diamond knife at −160 °C. Dry sections were picked up onto 600-mesh copper grids and, in order to enhance contrast, the microtomed sections were stained for 5–7 hours in vapor of I_2 crystals. Bright-field TEM was performed with JEOL-2000FX transmission electron microscope operating at an accelerating voltage of 200 kV.

2.6 Atomic force microscopy

Atomic force microscopy studies were performed with a scanning probe microscope Dimension 3100 AFM (Digital Instruments/Veeco Metrology Group). Bulk samples were cryomicrotomed at −160 °C to make a smooth surface for

the AFM imaging. All measurements were conducted at ambient conditions in tapping mode and height and phase images were recorded simultaneously. Initial amplitude of the probe oscillation and the set-point amplitude applied for imaging were chosen to maximize the image contrast between the soft P4VP(DBSA)$_{2.0}$ and the hard glassy PS domains.

2.7 UV-Vis spectroscopy

The transmission spectra for low molecular weight samples ($M_{n,\mathrm{PS}}$ = 42,100 g/mol, $M_{n,\mathrm{P4VP}}$ = 8,100 g/mol) were measured by Hitachi U-2000 double beam spectrophotometer in the wavelength range 200–1000 nm. Spectral diffuse reflectance and transmission of the high molecular weight samples were measured by utilizing the facilities at the Metrology Research Institute of Helsinki University of Technology in the wavelength range 300–950 nm. The angle of incidence was 8 degrees and light was collected with an integrating sphere detection system over the entire hemisphere; the specular component was included [29]. Spectral bandwidth of the spectrometer was set to 2.9 nm and the diameter of the measurement beam was adjusted to 8 mm for all the measurements.

Samples for optical measurements were slowly evaporated at 4 °C from dilute solution onto the quartz glass plate (low molecular weight samples) and additionally freestanding films were made for the transmission and reflectance measurements of high molecular weight samples. Thickness of samples was of the order of 100 μm (estimation is based on the sample weights and the substrate area).

3 Results and discussion

Pyridine and DBSA are a strong base and acid, respectively, and when they are mixed in solution, charge transfer from acid to a lone electron pair of pyridine is expected to take place, see *e.g.* [30]. On the other hand, recent studies with related compounds have shown that there is a competition between hydrogen bonding and protonation and that the equilibrium constant depends on the dielectric constant of the surrounding medium [31]. These interactions, in turn, make possible the formation of well-defined supramolecular structures when combined to the repulsion between the charged backbone and the hydrophobic alkyl tail (see Fig. 1).

Evidence for the interactions between the DBSA and the pyridines of PS-*block*-P4VP ($M_{n,\mathrm{PS}}$ = 238,100 g/mol, $M_{n,\mathrm{P4VP}}$ = 49,500 g/mol) was obtained from the FTIR analysis (Fig. 2). Pure PS-*block*-P4VP has an absorption band at *ca.* 1600 cm^{-1}, which results from the aromatic carbon-carbon stretching band of the phenyl groups of the PS-block and from the aromatic carbon-nitrogen stretching band of the unprotonated (*i.e.* free) pyridine rings within the P4VP-block (1596–1597 cm^{-1}). Pure DBSA also has an aromatic carbon-carbon stretching band of the phenyl groups at *ca.* 1600 cm^{-1}. Due to the protonation

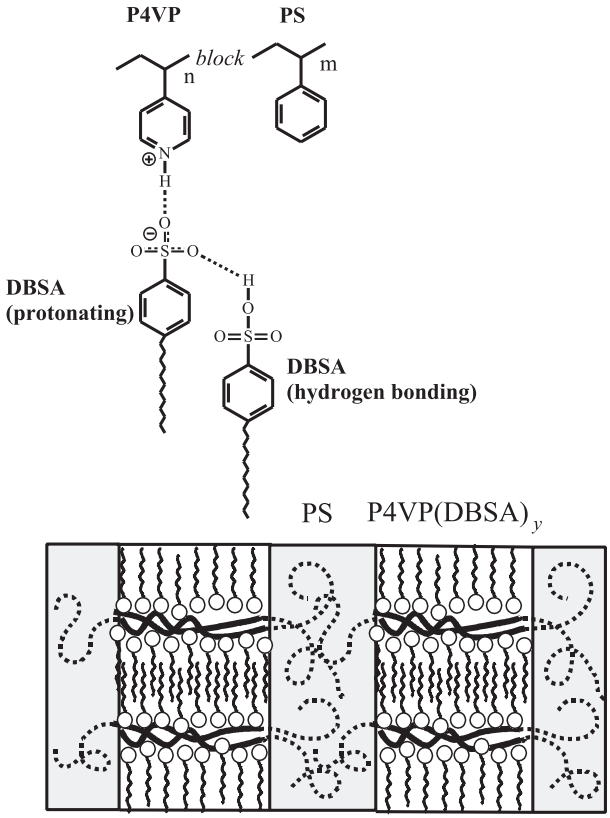

Fig. 1. The proposed scheme for the bonding between PS-*block*-P4VP and DBSA and structural hierarchy. Note that part of the DBSA molecules may be hydrogen bonded to P4VP instead of protonation.

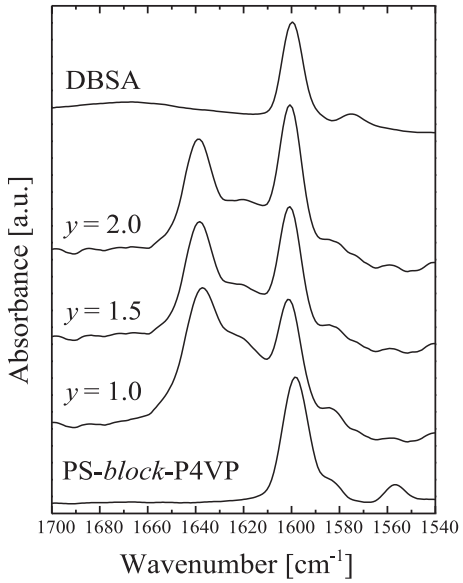

Fig. 2. FTIR absorption bands for DBSA, PS-*block*-P4VP(DBSA)$_y$ (y = 1.0−2.0), and PS-*block*-P4VP. The interaction between DBSA and block copolymer is seen as a shift of the aromatic carbon-nitrogen stretching band from 1597 cm^{-1} to *ca.* 1639 cm^{-1} corresponding to protonation. Another broad band is observed at *ca.* 1620 cm^{-1}, which may indicate hydrogen bonding.

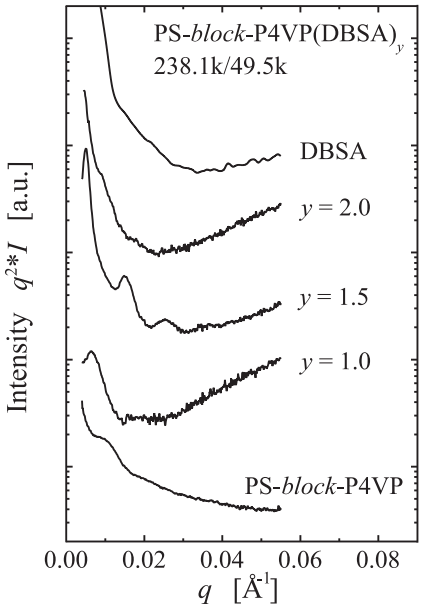

Fig. 3. X-ray scattering intensity patterns for DBSA, PS-*block*-P4VP(DBSA)$_y$ (y = 1.0, 1.5, and 2.0), and PS-*block*-P4VP in the $q < 0.056$ Å^{-1} region ($M_{n,\mathrm{PS}}$ = 238,100 g/mol, $M_{n,\mathrm{P4VP}}$ = 49,500 g/mol). The magnitude of the scattering vector is given by $q = (4\pi/\lambda)\sin\theta$ where 2θ is the scattering angle and $\lambda = 1.54$ Å.

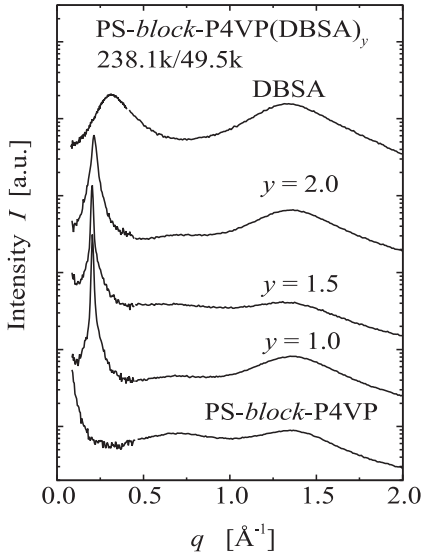

Fig. 4. X-ray scattering intensity patterns for DBSA, PS-*block*-P4VP(DBSA)$_y$, and PS-*block*-P4VP in the q = 0.08−2.00 Å^{-1} ($M_{n,\mathrm{PS}}$ = 238,100 g/mol, $M_{n,\mathrm{P4VP}}$ = 49,500 g/mol).

the carbon-nitrogen stretching band is expected to shift to higher wavenumbers. Indeed, a distinct absorption band is formed at *ca.* 1639 cm^{-1}, which corresponds to protonated P4VP [30]. However, there may be equilibrium between protonation and hydrogen bonding and another band observed for $y = 1.0$ as a shoulder at *ca.* 1620 cm^{-1} may be explained to result from strong hydrogen bonding between P4VP and DBSA instead of protonation. When the degree of complexation is increased, *i.e.* from $y = 1.0$ to 2.0, it seems that the shoulder is reduced suggesting that the equilibrium shifts even more towards protonation. Similar features are predicted, when the dielectric constant of the surrounding medium is increased [31]. Although the carbon-nitrogen stretching band of P4VP is shifted to higher wavenumbers due to interaction with DBSA, the relative absorbance at 1600 cm^{-1} increases with y. This is caused by an increased number of DBSA phenyl groups.

The structures and their periodicities were examined with X-ray scattering. In Figure 3, the intensity patterns are shown for the scattering vector range q = 0.004−0.056 Å^{-1}. DBSA does not show intensity maxima in this region, whereas PS-*block*-P4VP ($M_{n,\mathrm{PS}}$ = 238,100 g/mol, $M_{n,\mathrm{P4VP}}$ = 49,500 g/mol) has a shoulder at *ca.* 0.009 Å^{-1}. This corresponds to a length scale of *ca.* $L_p = 2\pi/q^* = 700$ Å, but a precise determination of the morphology couldn't be done due to the absence of higher order peaks. The complex with $y = 1.0$ has the first intensity maximum at $q^* = 0.0065$ Å^{-1} corresponding to $L_p = 970$ Å. For $y = 1.5$ a lamellar structure having the first intensity maximum at $q^* = 0.0050$ Å^{-1} with resolvable third, fifth and seventh order peaks is observed. This indicates a relatively well-developed lamellar structure with a long period of 1300 Å even without annealing and aligning. Lamellar structure is also expected because the weight fraction of PS in the complex is $w = 0.46$. Further increase to $y = 2.0$ leads to less well-developed order and only a fairly faint shoulder is observed at $q^* = 0.009$ Å^{-1}. Based on the TEM-micrograph (Fig. 5a), this is probably the second order maximum and the long period is about 1400 Å.

Note that even if the samples have not been aligned *e.g.* by roller casting techniques, and not even annealed, the materials containing DBSA show much better order than the uncomplexed PS-*block*-P4VP (see Fig. 3). This is an indirect manifestation of efficient plasticization by the DBSA combs.

X-ray scattering measurements were also performed at q-range (0.08–2.0 Å^{-1}) in order to investigate smaller structures resulting from the repulsion between the charged P4VP-chains and the nonpolar dodecyl side chain within the P4VP(DBSA)$_y$-domains (Fig. 4). Pure DBSA is an isotropic fluid and it has only a broad correlation hole maximum centered at $q^* = 0.31$ Å^{-1} corresponding to 20 Å. Note that hydronium salts of DBSA form lyotropic phases [32]. All complexes have the intensity maximum at 0.21 Å^{-1} (L_p = 30 Å). The morphology of these structures could not be determined due to the lack of higher order peaks. Note however, that as the first order peak is very narrow, we expect that there exists an ordered structure within the P4VP(DBSA)$_y$-layers. Based on geometrical arguments, we suggest that the structure is lamellar where the second order peak may be suppressed due to the nearly equal thicknesses of the alternating lamellae. That the long period of the inner structure is approximately constant as a function of y, deserves some

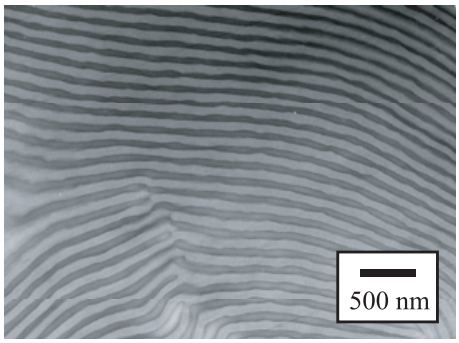

(a)

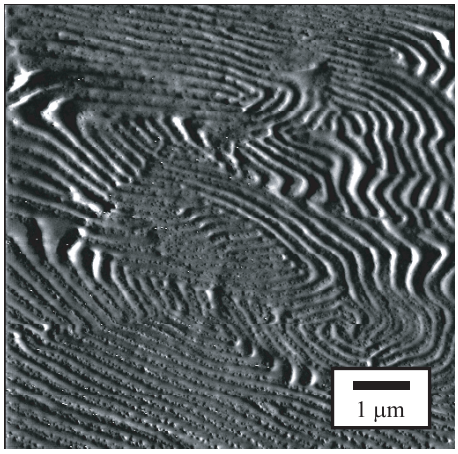

(b)

Fig. 5. (a) TEM micrograph of high molecular weight complex PS-*block*-P4VP(DBSA)$_{2.0}$ illustrating the lamellar structure with a long period *ca.* 1400 Å. The P4VP(DBSA)$_{2.0}$ phase shows dark in the image due to I_2 staining. Thicknesses of PS and P4VP(DBSA)$_{2.0}$ lamellae are almost equal, which qualitatively agrees with the P4VP(DBSA)$_{2.0}$ weight fraction $w = 0.60$. (b) AFM-phase image of PS-*block*-P4VP(DBSA)$_{2.0}$ illustrating the lamellar structure (the same sample as in Fig. 5a).

comments. Upon adding DBSA until $y = 1.0$ is reached, all pyridine rings can, in principle, be protonated, leading to P4VP(DBSA)$_{1.0}$. This first layer of DBSA contains sulphonate anions, which are hydrogen bonding acceptors, and further DBSA-molecules can be hydrogen bonded to it. That the long period of the smaller structure (P4VP(DBSA)$_y$) does not increase for $y > 1.0$, suggests that the P4VP chains have to stretch even further, implying that its lateral dimensions at the PS/P4VP(DBSA)$_y$ interface is reduced, which also leads additional stretching of the PS-blocks [33]. This would also explain the particularly large long periods observed in Figure 3.

Selected structures were also characterised using transmission electron microscopy (Fig. 5a) and atomic force microscopy (Fig. 5b). Figure 5a shows a micrograph of the high molecular weight complex PS-*block*-P4VP(DBSA)$_{2.0}$ which confirms the lamellar structure with a long period of *ca.* 1400 Å. This is in good agreement with the X-ray scattering results represented in Figure 3. Due to the I_2 staining, the P4VP(DBSA)$_{2.0}$ phase appear dark in the image. The thicknesses of the PS and P4VP(DBSA)$_{2.0}$ lamellae are almost equal which qualitatively agrees with the P4VP(DBSA)$_{2.0}$ weight fraction $w = 0.60$. The smaller structure was not observed in TEM. In Figure 5b, an atomic force micrograph of the same complex as in Figure 5a is presented, also indicating a lamellar structure.

Multilayer stacks constitute the simplest examples of photonic crystals. However, due to their 1D structure, they should not lead to complete photonic bandgap. Incident light is reflected from each interface between layers and the wavelength of reflected light depends on the optical thickness of structure. The refractive index contrast between the layers affects the amount of reflected light. In our case, the long periods of the high molecular weight block copolymer complexes are comparable to $\lambda/2n$ of light and the multilayer stack consists of alternating PS- and P4VP(DBSA)$_y$-layers. Refractive index contrast between polymer layers is normally small and also due to the lack of macroscopic orientation and the variation in long periods, a complete bandgap is difficult to fulfil using polymers.

Figure 6 depicts UV-Vis transmission and reflectance measurements. Pure DBSA and the uncomplexed PS-*block*-P4VP block copolymers are strongly absorbing below *ca.* 280 nm but they have relatively high transmission above it (Figs. 6a and b) and no bandgap is observed. Figure 6a shows that also the low molecular weight PS-*block*-P4VP(DBSA)$_y$ complexes had high transmission in visible range. This is due to the small periodicity because the weight fraction of DBSA, PS, and P4VP in these complexes are almost the same as in the high molecular weight complexes (see Figs. 6a and b), where the photonic bandgap is opened (see Fig. 6c).

High molecular weight PS-*block*-P4VP(DBSA)$_y$ with $y = 1.0$, in turn, starts to show a reduced transmission at *ca.* 400 nm, and for $y = 1.5$ the transmission spectra has a clear gap at 460 nm. The position of the gap qualitatively agrees with $\lambda/2n$ condition with long period of sample based on X-ray scattering studies (Fig. 3) (Typically the refractive index n of these kinds of polymers is of the order 1.5–1.6). PS-*block*-P4VP(DBSA)$_{2.0}$ also shows a gap but it is not that narrow. So far we do not know the reason for this behavior, but in this case the structure seems to be less developed, as indicated by the X-ray scattering results (Fig. 3). Both $y = 1.5$ and 2.0 were predominantly blue pearlescent to an observer viewing it in ambient, also suggesting a bandgap. Also reflectance measurements confirmed the formation of bandgap. Figure 6c depicts the reflectance curves for the same samples as in the Figure 6b. Complexes $y = 1.0$, 1.5, and 2.0 have the reflectance peaks at 370 nm, 460 nm, and 470 nm, respectively. The complex $y = 1.5$ has the highest and narrowest reflectance peak probably due to its well-developed structure, which was also confirmed by X-ray measurements (the relative width of the reflectivity peak, $\Delta\lambda/\lambda$, is *ca.* 0.20).

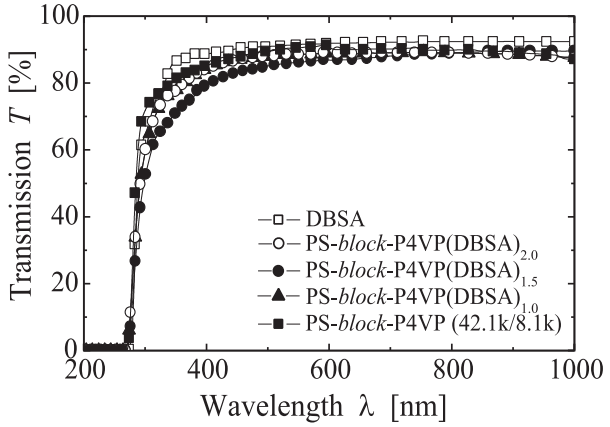

(a)

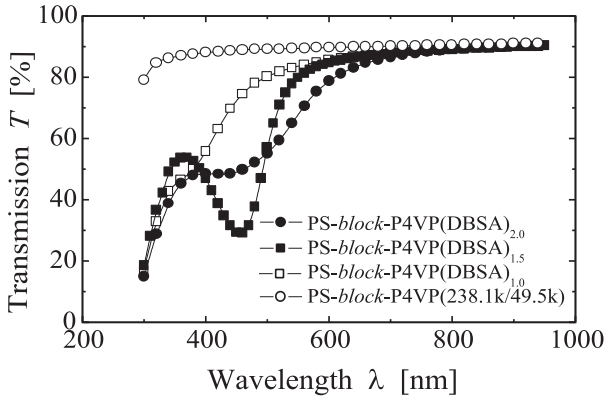

(b)

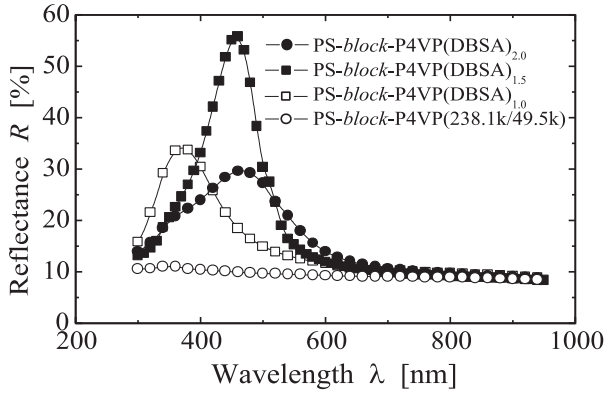

(c)

Fig. 6. UV-Vis transmission and reflectance graphs for DBSA, PS-*block*-P4VP, and PS-*block*-P4VP(DBSA)$_y$ with different molecular weights of the block copolymer. a) Low molecular weight, $M_{n,\mathrm{PS}} = 42{,}100$ g/mol, $M_{n,\mathrm{P4VP}} = 8{,}100$ g/mol, leading to short lamellar periodicities (measured from quartz substrate with Hitachi U-2000). b) Transmission and c) reflectance curves for high molecular weight block copolymer, which leads to very long periodicities in excess of 1000 Å enabling formation of bandgap.

The relatively narrow and incomplete bandgap results presumably from only a slight difference between refractive indexes of PS and P4VP(DBSA)$_y$ domains.

4 Conclusion

We have shown that complexes PS-*block*-P4VP(DBSA)$_y$ form hierarchically self-organized structures. Selecting a high molecular weight block copolymer, the long period increased up to *ca.* 1400 Å with increasing degree of complexation y as shown by X-ray scattering, TEM and AFM measurements. UV-Vis transmission and reflectance measurements indicate that a photonic bandgap was opened. The structure formation was relatively easy in such well-plasticized materials. The results encourage identifying further amphiphilic molecules of less acidic nature that are able to make strong bonding to block copolymer backbones. Tunability of the bandgap and the increase of refractive index difference between the domains are under investigations.

Tapio Mäkelä and Markku Ylilammi from VTT Microelectronics, Technical Research Centre of Finland, Saulius Nevas from Metrology Research Institute, and Matti Kaivola from Helsinki University of Technology are acknowledged for numerous discussions and experimental assistance. We acknowledge Volker Urban from ESRF/ID 2 for experimental assistance and discussions. C.K. Ober is acknowledged for discussion at the early stages. The financial support from the Academy of Finland and the National Technology Agency (Finland) are gratefully acknowledged. This work made use of UCSB Material Research Laboratory Central Facilities supported by the National Science Foundation under award No. DMR00-80034. This work was carried out in the Centre of Excellence of Finnish Academy ("Bio- and Nanopolymers Research Group", 77317).

References

1. J.D. Joannopoulos, R.D. Meade, J.N. Winn, *Photonic Crystals: Molding the Flow of Light* (Princeton University Press, Princeton, 1995)
2. T.F. Krauss, R.M. De La Rue, Progr. Quant. Electr. **23**, 51 (1999)
3. J.D. Joannopoulos, Nature **414**, 257 (2001)
4. *Materials Science Aspects of Photonic Crystals*, MRS Bulletin **26** (8) (2001)
5. *From Dynamics to Devices: Directed Self-Assembly of Colloidal Materials*, MRS Bulletin, **23** (10) (1998)
6. Y. Lu, Y. Yin, Y. Xia, Adv. Mater. **13**, 415 (2001)
7. S. John, K. Busch, J. Lightwave Technol. **17**, 1931 (1999)
8. K. Yoshino, Y. Kawagishi, M. Ozaki *et al.*, Jpn J. Appl. Phys. **38**, L786 (1999)
9. S. Satoh, H. Kajii, Y. Kawagishi *et al.*, Jpn J. Appl. Phys. **38**, L1475 (1999)
10. B. Gates, S.H. Park, Y. Xia, Adv. Mater. **12**, 653 (2000)
11. M. Müller, R. Zentel, T. Maka *et al.*, Chem. Mater. **12**, 2508 (2000)

12. A.A. Zakhidov, R.H. Baughman, Z. Iqbal *et al.*, Science **282**, 897 (1998)
13. Y.A. Vlasov, X.-Z. Bo, J.C. Sturm *et al.*, Nature **414**, 289 (2001)
14. D.J. Norris, Y.A. Vlasov, Adv. Mater. **13**, 371 (2001)
15. H. Miguez, F. Meseguer, C. López *et al.*, Adv. Mater. **13**, 393 (2001)
16. D. Wang, F. Caruso, Adv. Mater. **13**, 350 (2001)
17. Y. Fink, A.M. Urbas, M.G. Bawendi *et al.*, J. Lightwave Technol. **17**, 1963 (1999)
18. A. Urbas, Y. Fink, E.L. Thomas, Macromolecules **32**, 4748 (1999)
19. V.Z.-H. Chan, J. Hoffman, V.Y. Lee *et al.*, Science **286**, 1716 (1999)
20. A. Urbas, R. Sharp, Y. Fink *et al.*, Adv. Mater. **12**, 812 (2000)
21. A.C. Edrington, A.M. Urbas, P. DeRege *et al.*, Adv. Mater. **13**, 421 (2001)
22. S.A. Jenekhe, X.L. Chen, Science **283**, 372 (1999)
23. F.S. Bates, G.H. Fredrickson, Annu. Rev. Phys. Chem. **41**, 525 (1990)
24. I.W. Hamley, *The physics of block copolymers* (Oxford University Press, Oxford, 1998)
25. O. Ikkala, G. ten Brinke, Science **295**, 2407 (2002)
26. J. Ruokolainen, R. Mäkinen, M. Torkkeli *et al.*, Science **280**, 557 (1998)
27. J. Ruokolainen, M. Saariaho, O. Ikkala *et al.*, Macromolecules **32**, 1152 (1999)
28. H. Noguchi, in *Polymeric Materials Encyclopedia*, edited by J.C. Salamone, Vol. 5 (CRC Press, New York, 1996), p. 3392
29. S. Nevas, F. Manoocheri, Helsinki University of Technology, Metrology Research Institute Report **18**, 21 (2001)
30. O. Ikkala, J. Ruokolainen, G. ten Brinke *et al.*, Macromolecules **28**, 7088 (1995)
31. O. Lehtonen, J. Hartikainen, K. Rissanen *et al.*, J. Chem. Phys. 116, 2417 (2002)
32. B. Jönsson, B. Lindman, K. Holmberg *et al.*, *Surfactants and Polymers in Aqueous Solution* (John Wiley & Sons, New York, 1998)
33. V.V. Vasilevskaya, L.A. Gusev, A.R. Khokhlov *et al.*, Macromolecules **34**, 5019 (2001)